

1
2
3
4
5
6
7
8
9
10
11
12
13
14
15
16
17
18
19
20
21

The Role of the Ocean in the Global Atmospheric Budget of Acetone

Fischer, E. V.¹, Jacob, D. J.¹, Millet, D. B.², Yantosca, R. M.¹, and Mao, J.³

¹ School of Engineering and Applied Sciences, Harvard University, Cambridge, MA, USA

² Department of Soil, Water and Climate, University of Minnesota, St. Paul, MN, USA

³ Geophysical Fluid Dynamics Laboratory, Princeton, NJ, USA

Author to whom correspondence should be addressed:

Emily Fischer, Harvard University, Pierce Hall 110D, 29 Oxford Street, Cambridge, MA 02138
Phone: (603) 986-4241; Email: efischer@seas.harvard.edu

For Submission to: Geophysical Research Letters

October 20, 2011

22 **Abstract**

23 Acetone is one of the most abundant carbonyl compounds in the atmosphere and it plays
24 an important role in atmospheric chemistry. The role of the ocean in the global atmospheric
25 acetone budget is highly uncertain, with past studies reaching opposite conclusions as to whether
26 the ocean is a source or sink. Here we use a global 3-D chemical transport model (GEOS-Chem)
27 simulation of atmospheric acetone to evaluate the role of air-sea exchange in the global budget.
28 Inclusion of updated (slower) photolysis loss in the model means that a large net ocean source is
29 not needed to explain observed acetone in marine air. We find that a simulation with a fixed
30 seawater acetone concentration of 15 nM based on observations can reproduce the observed
31 global patterns of atmospheric concentrations and air-sea fluxes. The Northern Hemisphere
32 oceans are a net sink for acetone while the tropical oceans are a net source. On a global scale the
33 ocean is in near-equilibrium with the atmosphere. Prescribing an ocean concentration of acetone
34 as a boundary condition in the model assumes that ocean concentrations are controlled by
35 internal production and loss, rather than by air-sea exchange. An implication is that the ocean
36 plays a major role in controlling atmospheric acetone. This hypothesis needs to be tested by
37 better quantification of oceanic acetone sources and sinks.

38

39 **1. Introduction**

40 Acetone is the most abundant carbonyl compound in the atmosphere after formaldehyde.
41 In the upper troposphere, acetone photolysis is an important source of OH, the main atmospheric
42 oxidant. Acetone also affects the budget of nitrogen oxides by serving as a precursor for
43 peroxyacetyl nitrate (PAN), with complex implications for tropospheric ozone [*Singh et al.*,
44 1995]. Acetone is directly emitted by vegetation, biomass burning, and industry, and is also
45 produced in the atmosphere by oxidation of biogenic and anthropogenic volatile organic
46 compounds (VOCs). It is lost through oxidation by OH, photolysis, and surface uptake (Table
47 1).

48 A major uncertainty in the budget of atmospheric acetone is the role of the ocean.
49 Photochemical and biological processes in the ocean both produce and consume acetone
50 [*Nemecek-Marshall et al.*, 1995; *Sinha et al.*, 2007; *Zhou and Mopper*, 1997]. Atmospheric
51 acetone concentrations over the remote oceans are in the range 200 – 500 pptv [*Singh et al.*,
52 2000], only a factor 3 - 4 lower than over continental source regions. To account for this weak
53 gradient in the face of a relatively short (~15 days) atmospheric lifetime, *Jacob et al.* [2002]
54 hypothesized a large oceanic emission of acetone in simulations with the GEOS-Chem global
55 chemical transport model (CTM). Since then, measurements of the quantum yield for acetone
56 photolysis have led to upward revision of the atmospheric lifetime for acetone [*Blitz et al.*, 2004].
57 In addition, field observations have shown that the ocean can be either a source or a sink of
58 acetone [*Marandino et al.*, 2005; *Sinha et al.*, 2007; *Taddei et al.*, 2009; *Williams et al.*, 2004].
59 Here we use GEOS-Chem to integrate these new experimental data into an improved
60 understanding of the role of the ocean in the global budget of atmospheric acetone.

61 **2. Methods**

62 We use the GEOS-Chem global 3-D CTM driven by NASA/GEOS-5 assimilated
63 meteorological data (version 9.01.01, www.geos-chem.org) to simulate the global atmospheric
64 distribution of acetone. The GEOS-5 fields have $0.5^\circ \times 0.67^\circ$ horizontal resolution, 47 levels in
65 the vertical, and 3 – 6 hour temporal resolution. We degrade horizontal resolution to $2^\circ \times 2.5^\circ$
66 for input into GEOS-Chem. We use a 1-year simulation for 2006, with a 1-year spin-up to
67 remove the effect of initial conditions.

68 Sources of acetone include direct emissions from biogenic, anthropogenic, and biomass
69 burning sources, as well as the atmospheric oxidation of organic precursors (Table 1). The
70 ensemble of sources is described by *Jacob et al.* [2002] and updates are described below. We
71 use the RETRO (Reanalysis of the TROpospheric chemical composition) emission inventory for
72 anthropogenic emissions of acetone and of the isoalkane precursors [*van het Bolscher et al.*,
73 2008]. The RETRO emission inventory is for 2000, and we scale it to 2006 with activity factors
74 from *van Donkelaar et al.* [2008]. We use 2006 GFED2 monthly biomass burning emissions for
75 acetone and the isoalkanes [*van der Werf et al.*, 2009]. Terrestrial biogenic emissions of acetone
76 from metabolism and decay are calculated locally using the Model of Emissions of Gases and
77 Aerosols from Nature (MEGAN v2.0) [*Guenther et al.*, 2006]. Acetone production from the
78 atmospheric oxidation of biogenic monoterpenes and 2-methyl-3-buten-2-ol is calculated using
79 emissions from MEGAN and acetone yields from *Jacob et al.* [2002].

80 Losses for acetone in the model include oxidation by OH, photolysis, and deposition.
81 Exchange with the ocean is discussed below. We use a rate constant $k = 1.33 \times 10^{-13} + 3.28 \times$
82 $10^{-11} \exp[-2000/T] \text{ cm}^3 \text{ molecule}^{-1} \text{ s}^{-1}$ for the oxidation of acetone by OH [*Sander et al.*, 2011].
83 Photolysis of acetone is computed using absorption cross sections and pressure-dependent
84 quantum yields from *Blitz et al.* [2004], and local actinic fluxes from the Fast-JX radiative

85 transfer scheme [Wild *et al.*, 2000] as implemented in GEOS-Chem by Mao *et al.* [2010]. We
86 assume a dry deposition velocity of 0.1 cm s^{-1} for ice-free land as in Jacob *et al.* [2002].

87 There is evidence that the ocean mixed layer is a large acetone reservoir, containing ~5
88 times the atmospheric burden [Williams *et al.*, 2004]. We compile in Table 2 literature values
89 for observed surface seawater concentrations and air-sea fluxes. The processes controlling
90 acetone concentrations in seawater are uncertain. Production can take place by photo-
91 degradation of dissolved organic matter [Zhou and Mopper, 1997] and directly by phytoplankton
92 and bacteria [Nemecek-Marshall *et al.*, 1995]. Loss can take place by photo-degradation or
93 biotic consumption [Mopper and Stahovec, 1986; Nemecek-Marshall *et al.*, 1995]. Two recent
94 field campaigns support a biologically mediated acetone source in seawater. Sinha *et al.* [2007]
95 measured the air-sea flux of acetone while also monitoring phytoplankton. They found
96 systematic upward fluxes in the presence of both strong daylight and biological activity. Taddei
97 *et al.* [2009] also observed upward acetone fluxes in phytoplankton bloom areas in the South
98 Atlantic.

99 For implementation in GEOS-Chem we assume a fixed seawater acetone concentration of
100 15 nM, based on the data in Table 2. The data do not show evident seasonal or spatial patterns.
101 By setting a fixed seawater concentration we assume implicitly that acetone in the ocean is
102 controlled by internal sources and sinks, rather than exchange with the atmosphere. There is
103 some support for this argument based on analogy with methanol. Williams *et al.* [2004] reported
104 a sharper vertical gradient for acetone than methanol in the ocean mixed layer, implying a shorter
105 lifetime for acetone. Heikes *et al.* [2002] estimated an ocean mixed lifetime for methanol of 3
106 days against bacterial uptake, and Williams *et al.* [2004] estimated an ocean mixed layer burden
107 of 15.9 Tg for acetone. Assuming an upper limit of 3 days for the acetone lifetime in the ocean

108 mixed layer, a minimum source of 2000 Tg a^{-1} would be needed to sustain the ocean mixed layer
109 burden. This is much larger than the atmospheric source of acetone (Table 1), and thus the
110 acetone concentration in the ocean is likely internally controlled.

111 We calculate air-sea fluxes of acetone locally in GEOS-Chem on the basis of a seawater
112 concentration of 15 nM by applying the two-film model of *Liss and Slater* [1974], with liquid
113 and gas-phase transfer velocities following *Nightingale et al.* [2000] and *Johnson* [2010]
114 respectively. The Henry's law equilibrium constant for acetone is 27 M atm^{-1} [*Benkelberg et al.*,
115 1995]. Equilibrium with a seawater concentration of 15 nM implies atmospheric acetone mixing
116 ratios of 220 pptv and 550 pptv at 283 K and 298 K respectively. Observed acetone mixing
117 ratios in the marine boundary layer are typically in that range [*Singh et al.*, 2000], so the ocean
118 can be either a net source or sink for acetone depending on the local atmospheric concentration
119 and surface temperature.

120 **3. Global Atmospheric Distribution of Acetone**

121 Figure 1 shows the simulated acetone mixing ratios in three altitude ranges and for two
122 seasons. Mean observations from aircraft missions, ship cruises, and surface sites are overlaid as
123 circles. The observations are generally for years other than 2006 but we expect that interannual
124 variability is small relative to other aspects of variability. Figure 2 presents the simulated annual
125 mean acetone air-sea acetone fluxes. The ocean parameterization produces a weak global sink of
126 2 Tg a^{-1} , but the net flux varies geographically and seasonally. The ocean is a net sink at
127 northern latitudes but a net source between 20°N and 40°S . At high southern latitudes the
128 atmosphere and ocean are near equilibrium during summer and the ocean is a weak sink during
129 winter. Comparison with observed fluxes is discussed below.

130 The atmospheric simulation shows no systematic bias compared to the observations in Figure
131 1 and provides in general a good representation of observed latitudinal and seasonal variability as
132 well as land-ocean gradients. It performs similarly to the simulation of *Jacob et al.* [2002],
133 which used Bayesian optimization to match observations. A major difference is that we do not
134 need to invoke a large global ocean source in order to explain the observations in marine air.
135 This is because our mean atmospheric lifetime of acetone against chemical sinks (photolysis and
136 reaction with OH) is 39 days, compared to 19 days in *Jacob et al.* [2002], reflecting the lower
137 photolysis quantum yields from *Blitz et al.* [2004]. Thus we have more transport of continental
138 acetone to the oceans. The tropical oceans remain a net source of acetone in our simulation,
139 which is consistent with the limited data of Table 2 [*Williams et al.*, 2004] and can account for
140 the relatively high acetone concentrations observed over the tropical Pacific [*Singh et al.*, 2001].
141 Unlike at northern mid-latitudes, aircraft vertical profiles over the tropical oceans do not show
142 depletion of acetone in the marine boundary layer relative to the free troposphere above [*Singh et*
143 *al.*, 2001].

144 Figure 2 shows the strongest ocean sink downwind of the Northern Hemisphere continents
145 where high atmospheric acetone concentrations are coupled with strong wind speeds and cold
146 temperatures. We explain in this manner the observed acetone depletion in the marine boundary
147 layer relative to the free troposphere over the North Pacific [*Singh et al.*, 2003] and data over the
148 Northwest Atlantic showing the ocean to be a sink for acetone in continental outflow [*Mao et al.*,
149 2006]. Based on acetone / CO ratios from the INDOEX and MINOS field campaigns, *de Reus et*
150 *al.* [2003] speculated that that the ocean serves a sink for acetone in polluted regions and a
151 source in clean air masses. Our global results are consistent with this view. *Marandino et al.*
152 [2005] find a stronger ocean sink than the model over the northwest Pacific (Figure 2) but their

153 atmospheric acetone observations were very high (averaging 1.05 ppbv) and apparently
154 anomalous relative to the other data in Figure 1.

155 The lowest tropospheric concentrations simulated by the model are over the Southern
156 Ocean, reflecting the remoteness from sources and the cold ocean temperatures. There the mean
157 concentration is 0.2 ppbv and the ocean is a weak net sink. These results are consistent with
158 cruise data in the Southern Ocean between South Africa and Chile [Taddei *et al.*, 2009].

159 **4. Atmospheric Budget**

160 Table 1 summarizes our global atmospheric budget of acetone and compares it to
161 previous estimates. We separate the ocean source and sink terms since we view them as
162 independent. We find a global source of acetone of 146 Tg a⁻¹ including 80 Tg a⁻¹ from the
163 oceans, 33 Tg a⁻¹ from the terrestrial biosphere, and 26 Tg a⁻¹ from the atmospheric oxidation of
164 isoalkanes. We calculate a mean tropospheric lifetime of 14 days with ocean uptake contributing
165 56 % of the sink; reaction with OH, photolysis, and land uptake contribute 23 %, 13 %, and 8 %
166 of the sink respectively.

167 The updated acetone photolysis rates triple the tropospheric lifetime of acetone against
168 photolysis relative to *Jacob et al.* [2002] and reverse the relative importance of oxidation versus
169 photolysis. We estimate an atmospheric burden of 5.6 Tg, which is larger than the estimate by
170 *Jacob et al.* [2002] (3.8 Tg), because our weaker photolysis sink increases the burden in the
171 upper troposphere. This is consistent with observations, as shown in Figure 1. *Arnold et al.*
172 [2005] previously found with the TOMCAT CTM that the updated (slower) photolysis loss
173 increases the acetone tropospheric burden by 50%.

174 Separation of the ocean source and sink in our budget suggests that the ocean exerts a
175 major control on the abundance of atmospheric acetone. We find that on a global scale the

176 atmosphere is in near equilibrium with the ocean (the net ocean sink of 2 Tg a^{-1} , corresponding to
177 an ocean saturation ratio of 0.98, is within the uncertainty of the other source and sink terms).
178 However there are coherent regions where the ocean is either a net sink or a net source,
179 depending on the atmospheric acetone concentration and temperature. *Marandino et al.* [2005]
180 proposed that the ocean is a large global net sink based on extrapolation of their measurements in
181 the North Pacific Ocean, but as pointed out above their measurements were taken under
182 conditions of anomalously high acetone concentrations in surface air. The other flux
183 measurements in Table 2 do not support this extrapolation. Better quantification of the sources
184 and sinks of acetone in the oceans, including seasonal and geographical variability, is critical to
185 improve our understanding of the budget of atmospheric acetone.

186 **Acknowledgments:** This work was supported by the NASA Atmospheric Composition
187 Modeling and Analysis Program. Support for Emily V. Fischer was provided by the NOAA
188 Climate and Global Change Postdoctoral Fellowship Program, administered by the University
189 Corporation for Atmospheric Research, and by a Harvard University Center for the Environment
190 Postdoctoral Fellowship.

191

192 **Tables**193 **Table 1:** Global atmospheric acetone budget

	This Work	Jacob et al. [2002]	Other Estimates ^a
Inventory, Tg	5.6	3.8	3.8 – 7.2
Sources, Tg a⁻¹			
<i>Emissions</i>			
Anthropogenic	0.73 ^b	1.1 ± 0.5	1.1 - 2
Open biomass burning	2.8	4.5 ± 1.6	2.4 – 9
Terrestrial Biosphere	32	35 ± 10	20 – 172
<i>Atmospheric Production</i>			
Oxidation of isoalkanes (mainly anthropogenic)	26 ^c	21 ± 5	16 – 28
Oxidation of biogenic VOCs	5	7 ± 3	7
Sinks, Tg a⁻¹			
Oxidation by OH	33	27	18 - 27
Photolysis	19	46	9 - 22
Land uptake	12	9	9 - 19
Net Ocean exchange, Tg a⁻¹^d	-2	13 ± 6	-62 – 2.5
Gross source	80	NA	NA
Gross sink	82	NA	NA

194

195 ^a *Arnold et al.* [2005], *Singh et al.* [2003, 2004], *Potter et al.* [2003], *Marandino et al.* [2006],
 196 *Sinha et al.* [2007], *Pozzer et al.* [2010], *Elias et al.* [2011].

197 ^b Including biofuel use.

198 ^c Including 22 Tg a⁻¹ from propane and 4 Tg a⁻¹ from the higher alkanes.

199 ^d Positive values indicate upward fluxes.

200

201

202

203

204

205

206

207 **Table 2:** Measurements of acetone concentrations in surface seawater and air-sea fluxes^a.

Period	Location	Concentration (nM)	Flux ^b (ng m ⁻² s ⁻¹)	Reference
Mar 1989	Bahamas	3 – 15 ^c	-2.8 – 1.0* ^c	<i>Zhou and Mopper</i> [1997]
Oct – Nov 2002	Tropical Atlantic	17.6 ± 8.1	7.8*	<i>Williams et al.</i> [2004]
May -Jul 2004	W. Pacific (mid-latitude)	13.6 ± 3.0	-10.2 ^d , -7.4*	<i>Marandino et al.</i> [2005]
May -Jul 2004	W. Pacific (equatorial)	13.9 ± 11.7	-2.6 ^d , 1.1*	<i>Marandino et al.</i> [2005]
Jun – Jul 2004	North Atlantic	< 9.6	----	<i>Hudson et al.</i> [2007]
May – Jun 2005	Norwegian fjord	----	0.21	<i>Sinha et al.</i> [2007]
Jan – Feb 2007	S. Atlantic (bloom)	----	0.67	<i>Taddei et al.</i> [2009]
Jan 2007	S. Atlantic (non-bloom)	----	~ -1.0 – 0.2 ^e	<i>Taddei et al.</i> [2009]
Jul – Aug 2008	Northwest Pacific	19.0 ± 4.4	----	<i>Kameyama et al.</i> [2010]

208 ^a Values are means ± standard deviation unless otherwise noted.

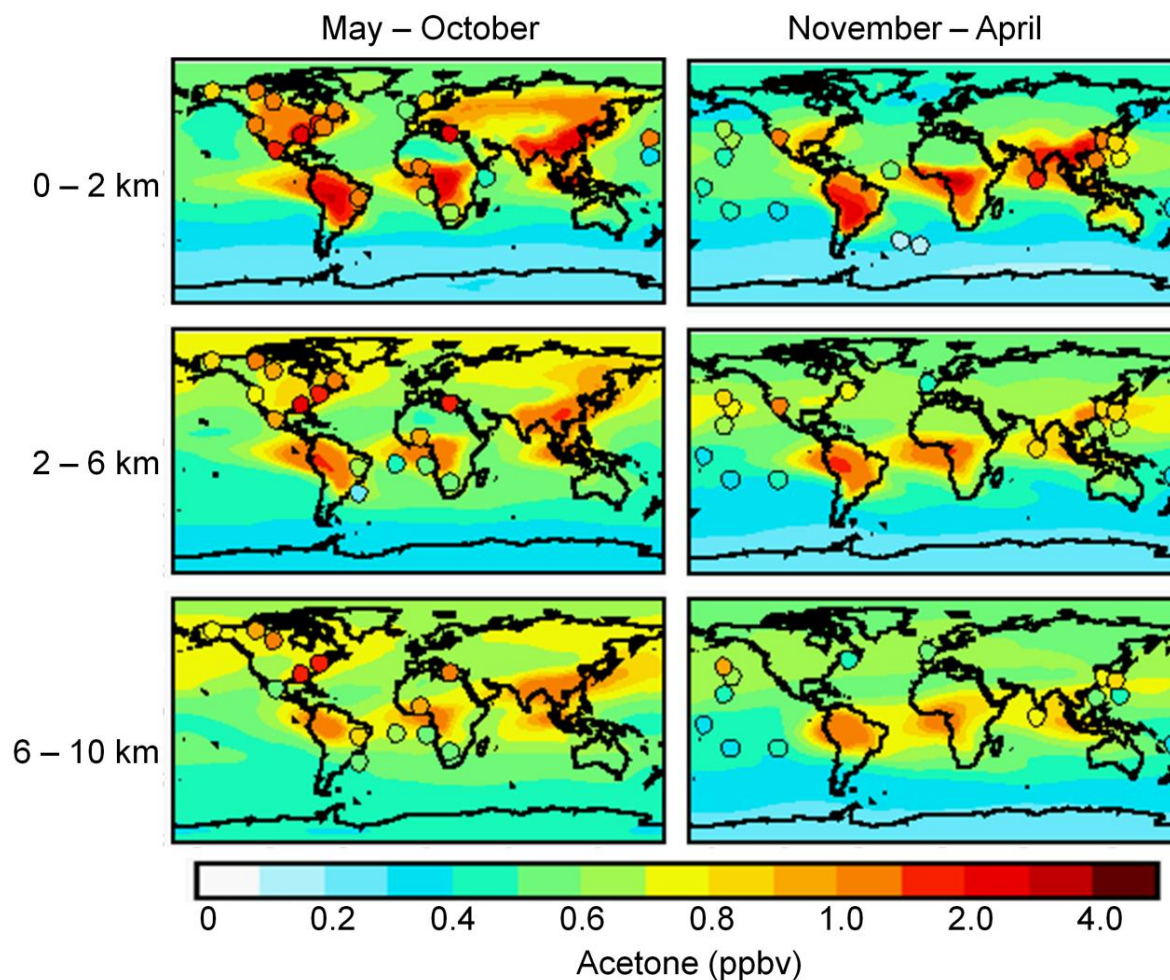
209 ^b Fluxes were either directly measured by eddy covariance or mesocoms, or were inferred from
 210 the measured saturation ratios. The latter are indicated by asterisks. Positive fluxes are upward.

211 ^c Ranges of concentrations and inferred fluxes. The authors reported a flux of 15.7 ng m⁻² s⁻¹
 212 based on an acetone concentration of 55 nM in the surface micro-layer. We repeated their flux
 213 calculations using their measured seawater concentrations.

214 ^d The authors reported a discrepancy between the fluxes measured by eddy covariance and
 215 inferred from saturation ratios. Both are shown here. All measured fluxes were downward, but
 216 the range of saturation ratios (0.35 - 6.5), implied both upward and downward fluxes.

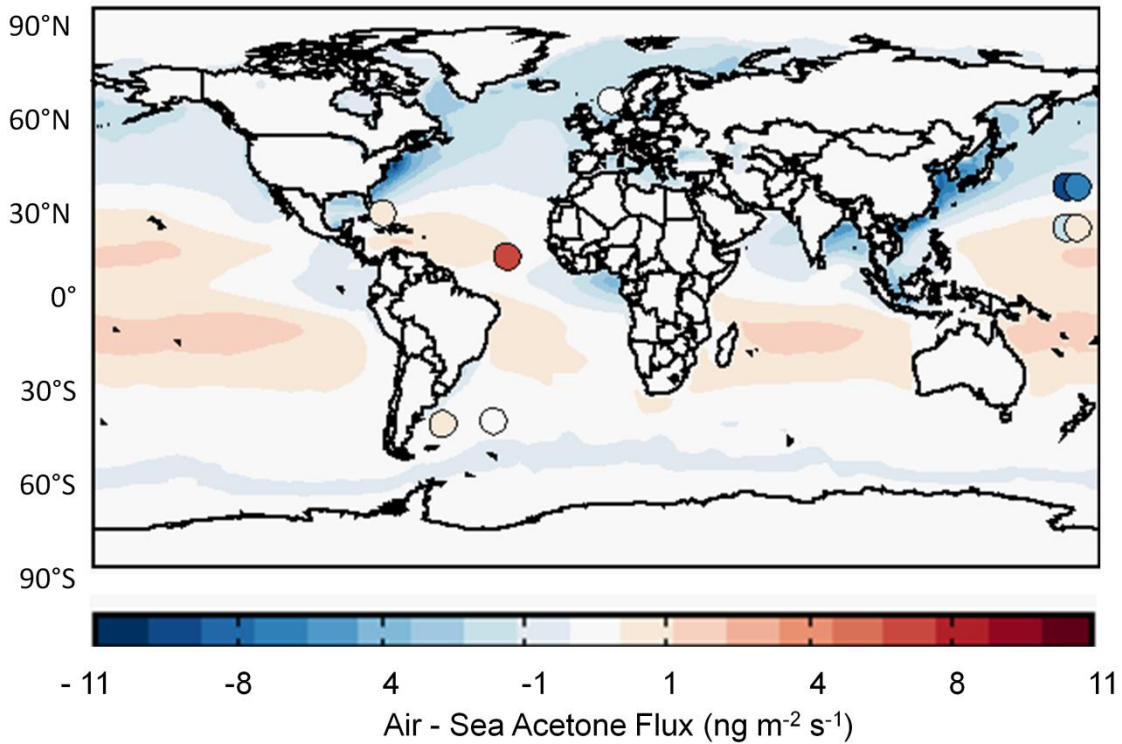
217 ^e *Taddei et al.* [2009] report “near zero, negative or highly variable low acetone fluxes” in non-
 218 bloom conditions. They do not report a mean value for non-bloom conditions, thus a range is
 219 given here based on DOY 28 – 30 in their Figure 4.

220
 221
 222
 223
 224
 225



227
 228 **Figure 1:** Simulated and observed global distribution of atmospheric acetone for two seasons
 229 and three altitude bins. Simulated mixing ratios are for 2006 and are shown as solid contours.
 230 Filled circles are mean observations in different years from aircraft missions, ship cruises and
 231 surface sites [*de Gouw et al.*, 2001; *de Gouw et al.*, 2006; *Hornbrook et al.*, 2011; *Jacob et al.*,
 232 1996; *Lelieveld et al.*, 2002; *Lewis et al.*, 2005; *Mao et al.*, 2006; *Marandino et al.*, 2005;
 233 *Murphy et al.*, 2010; *Singh et al.*, 2000; *Singh et al.*, 2009; *Singh et al.*, 2001; *Singh et al.*, 1994;
 234 *Singh et al.*, 2004; *Warneke and de Gouw*, 2001; *Williams et al.*, 2004]. Data for aircraft
 235 missions have been averaged over regionally coherent regions as in *Jacob et al.* [2002] with the
 236 addition of more recent missions. Data from ship cruises are primarily the averages reported in

237 the literature. Circles are placed at the mean latitude and longitude of the observations.
238 Auxiliary Table 1 gives details of the observations. Auxiliary Figures 1 and 2 show comparisons
239 with the aircraft vertical profiles.
240



241

242 **Figure 2.** Simulated annual mean air-sea fluxes of acetone for 2006, and mean observed air-sea
 243 fluxes (Table 2, Column 3). Positive values indicate a net flux from the sea to the air.

244 *Marandino et al.* [2005] report a discrepancy between the flux calculated from the saturation
 245 ratio and that measured by eddy covariance. Both are shown here over the western Pacific, with
 246 the measured fluxes plotted to the west of the calculated fluxes. There is seasonal variation to
 247 the net air-sea fluxes, and Auxiliary Figure 3 presents the fluxes for January and July.

248

249

250

251

252

253

254

255 **Auxiliary Materials**

256 **Auxiliary Table 1:** Observations of acetone compared to model output in Figure 1. Region
 257 numbers for aircraft data refer to Auxiliary Figure 1.

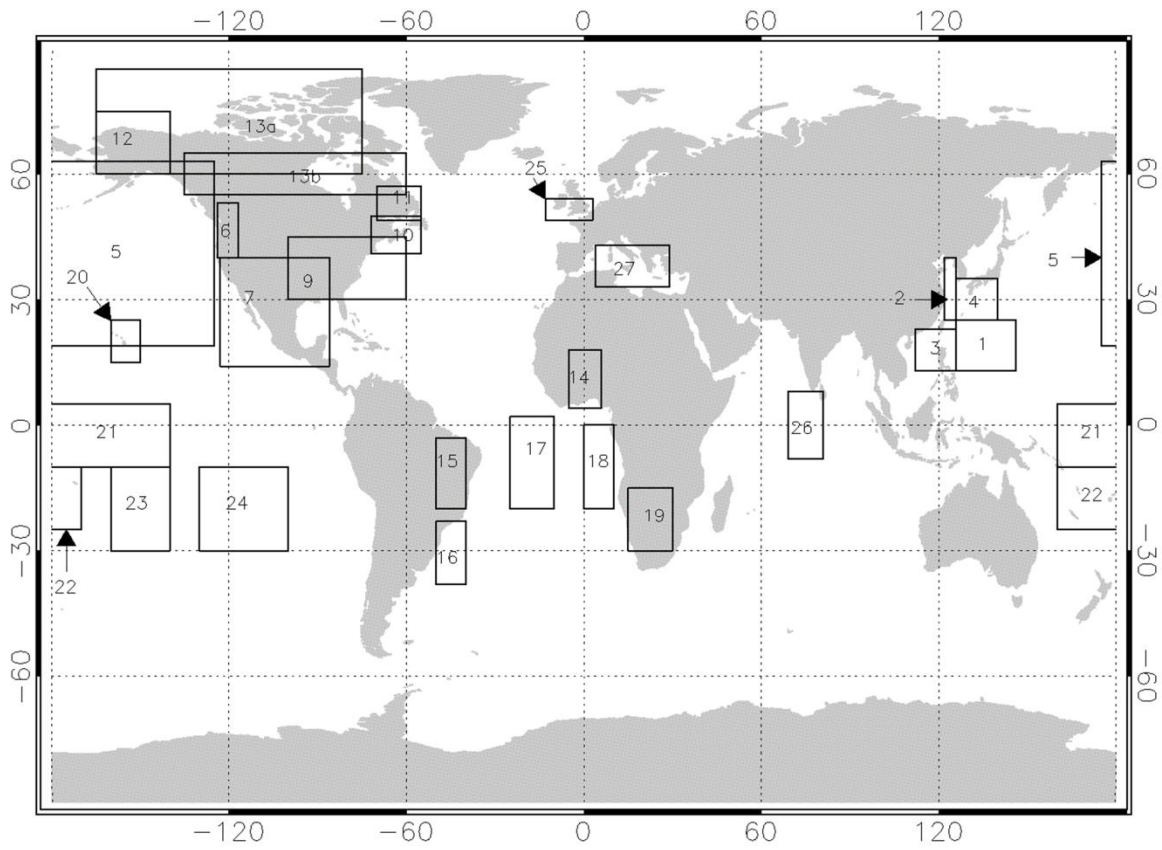
	Time Period	Map Region(s)	Source
Aircraft Missions			
TRACE-P, Western Pacific	Mar– Apr 2001	1 - 4	<i>Singh et al.</i> [2004]
INTEX-B, Eastern Pacific	Mar – May 2006	5	<i>Singh et al.</i> [2009]
IMPEX North Western U.S.	Mar – May 2006	6	T. Karl
MILAGRO, Mexico	Mar – May 2006	7	<i>Singh et al.</i> [2009]
INTEX-NA, Eastern U.S. ^a	Jul – Aug 2004	8 - 9	<i>de Gouw et al.</i> [2006]
SONEX, North Atlantic	Oct – Nov 1997	10,25	<i>Singh et al.</i> [2000]
Able-3B, Eastern Canada	July – Aug 1990	11	<i>Singh et al.</i> [1994]
ARCPAC, N. American Arctic	Apr – Jul 2008	12	J. de Gouw, C. Warneke
ARCTAS, N. American Arctic	Apr – Jul 2008	13	<i>Hornbrook et al.</i> [2010]
AMMA, West Africa	Jul – Aug 2006	16	<i>Murphy et al.</i> [2010]
Trace-A (TA), South Atlantic	Sept – Oct 1992	15 - 19	<i>Jacob et al.</i> [1996]
PEM-Tropics B (PEMTB)	Mar – Apr 1999	20 - 24	<i>Singh et al.</i> [2001]
INDOEX, Indian Ocean	Feb – Mar 1999	26	<i>de Gouw et al.</i> [2001]
MINOS, Mediterranean	Aug 2001	27	<i>Lelieveld et al.</i> [2002]
Ship Cruises			
Tropical Atlantic	Oct – Nov 2002		<i>Williams et al.</i> [2004]
Western Pacific	May – Jul 2004		<i>Marandino et al.</i> [2005]
OOMP, South Atlantic ^b	Jan – Mar 2007		<i>Taddei et al.</i> [2009]
Pelagai, Indian Ocean	April 2000		<i>Warneke and de Gouw</i> [2001]
Marine Layer Surface Sites			
Appledore Island	Jul – Aug 2004		<i>Mao et al.</i> [2006]
Mace Head	Jul – Sept 2002		<i>Lewis et al.</i> [2005]

258
 259 ^a Aircraft observations have been filtered to exclude biomass burning plumes, as diagnosed by
 260 HCN > 500 pptv, since the model does not have the resolution to capture those plumes and they
 261 would otherwise bias the mean.

262 ^b Data from two legs of the OOMP campaign are shown separately in Figure 1. The mean
 263 value is plotted for the first leg of the cruise from South Africa to Chile. The second leg of the
 264 plume, from Chile to South Africa, traversed more southern latitudes. The median is plotted for

265 the second leg of the cruise, where the median (147 pptv) was much different than the mean (883
266 pptv), which is biased by a few very acetone high mixing ratios.

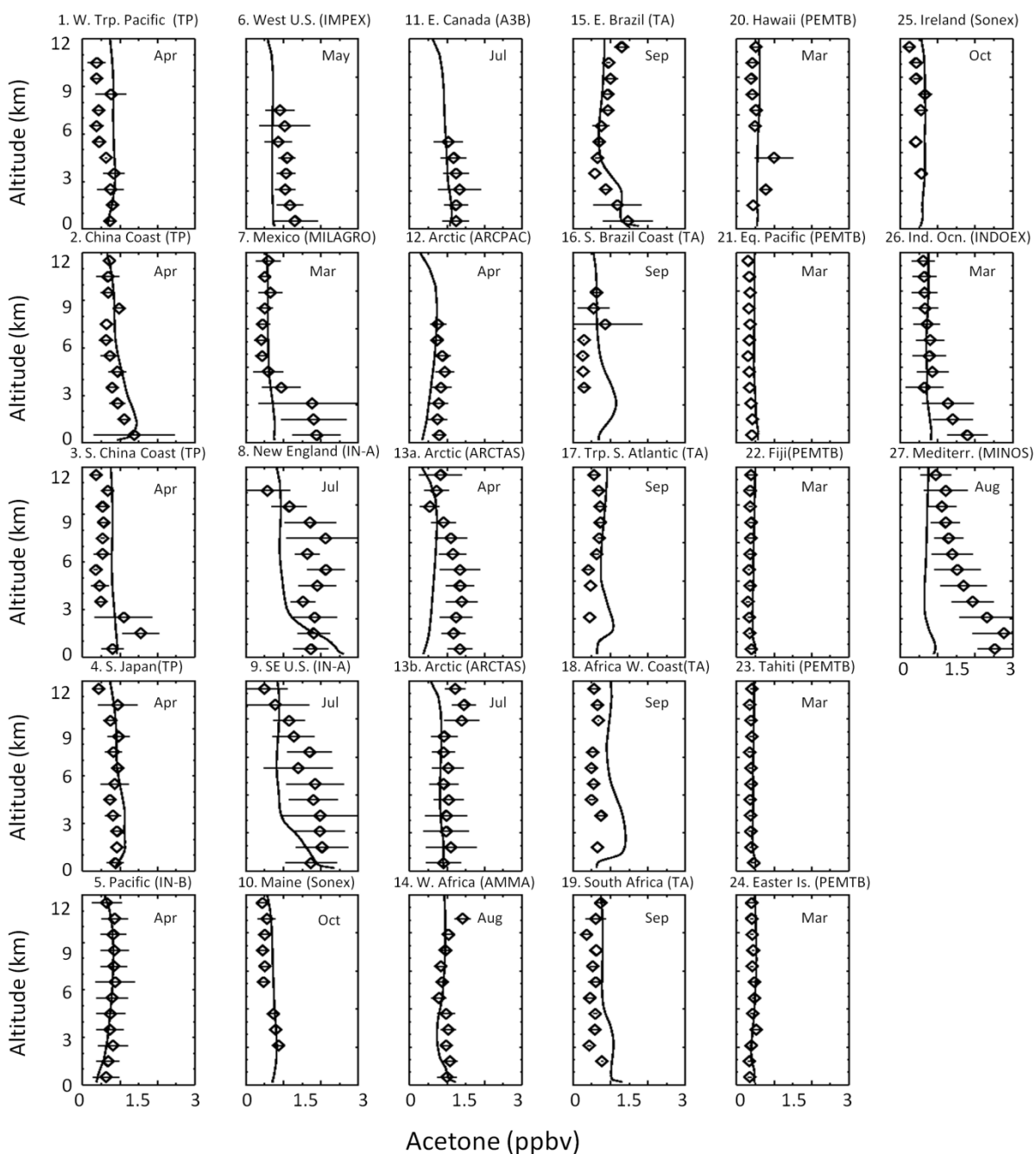
267



268

269 **Auxiliary Figure 1:** Map with boxes surrounding coherent regions used to average the aircraft

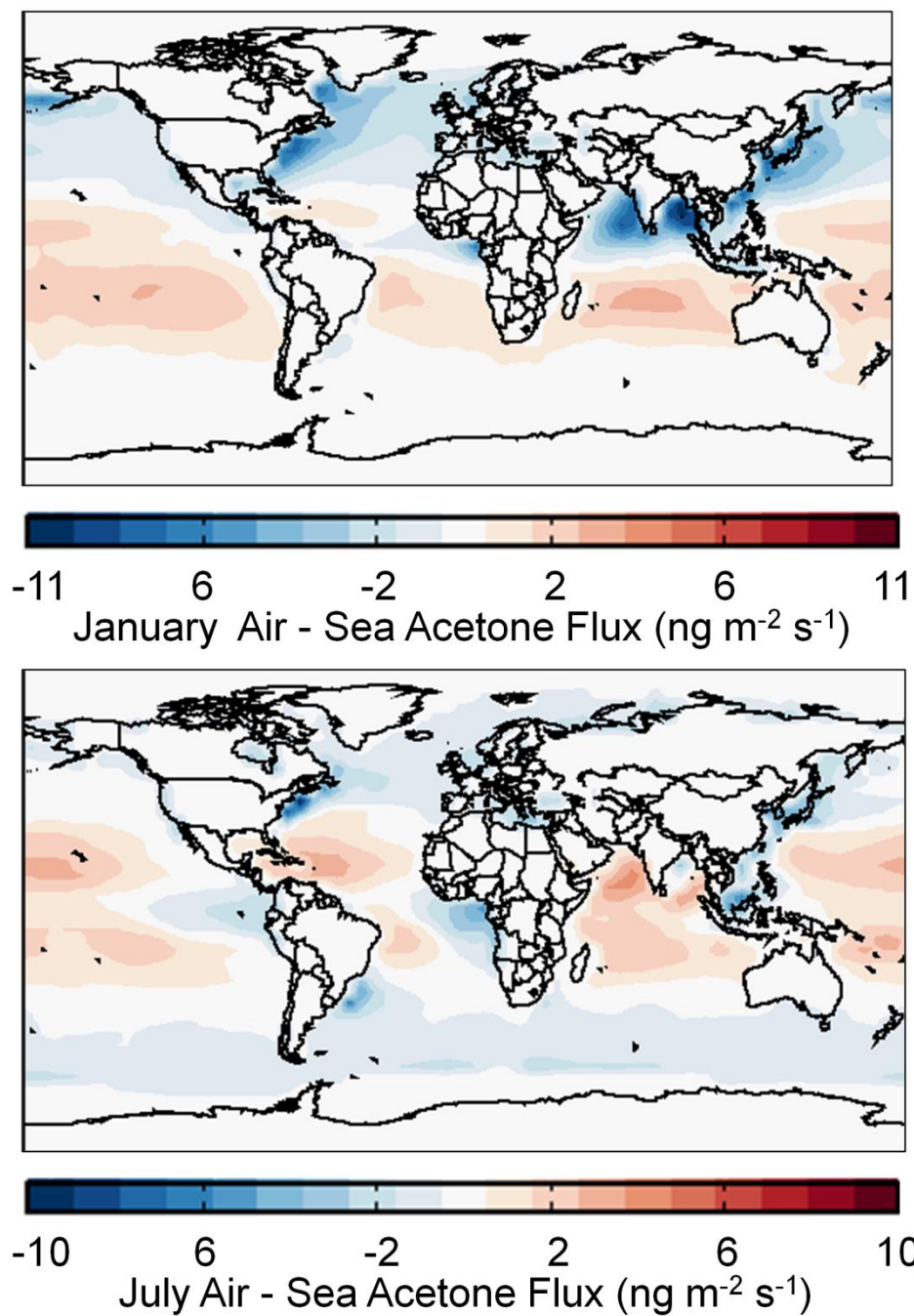
270 observations shown in Auxiliary Figure 2.



271

272 **Auxiliary Figure 2.** Comparison of simulated and observed vertical profiles of acetone
 273 concentrations from recent aircraft missions. The INTEX-NA data has been filtered to remove
 274 the largest biomass burning plumes using flight logs and HCN observations > 500 pptv.

275



276
277 **Auxiliary Figure 3.** Simulated annual mean air-sea fluxes of acetone for January and July 2006.
278 Positive values indicate a net flux from the sea to the air.

279
280
281

282 **References**

- 283 Arnold, S. R., et al. (2005), A three-dimensional model study of the effect of new temperature-dependent
284 quantum yields for acetone photolysis, *J. Geophys. Res.*, *110*(D22), D22305,
285 doi:10.1029/2005jd005998.
286
287
- 288 Benkelberg, H. J., et al. (1995), Henry's law coefficients for aqueous solutions of acetone, acetaldehyde
289 and acetonitrile, and equilibrium constants for the addition compounds of acetone and
290 acetaldehyde with bisulfite, *Journal of Atmospheric Chemistry*, *20*(1), 17-34,
291 doi:10.1007/bf01099916.
292
293
- 294 Blitz, M. A., et al. (2004), Pressure and temperature-dependent quantum yields for the photodissociation
295 of acetone between 279 and 327.5 nm, *Geophys. Res. Lett.*, *31*(6), L06111,
296 doi:10.1029/2003gl018793.
297
298
- 299 de Gouw, J. A., et al. (2001), Overview of the trace gas measurements on board the Citation aircraft
300 during the intensive field phase of INDOEX, *J. Geophys. Res.*, *106*(D22), 28453-28467,
301 doi:10.1029/2000jd900810.
302
303
- 304 de Gouw, J. A., et al. (2006), Volatile organic compounds composition of merged and aged forest fire
305 plumes from Alaska and western Canada, *J. Geophys. Res.*, *111*(D10), D10303,
306 doi:10.1029/2005jd006175.
307
308
- 309 de Reus, M., et al. (2003), On the relationship between acetone and carbon monoxide in different air
310 masses, *Atmos. Chem. Phys.*, *3*(5), 1709-1723, doi:10.5194/acp-3-1709-2003.
311
312
- 313 Guenther, A., et al. (2006), Estimates of global terrestrial isoprene emissions using MEGAN (Model of
314 Emissions of Gases and Aerosols from Nature), *Atmos. Chem. Phys.*, *6*(11), 3181-3210,
315 doi:10.5194/acp-6-3181-2006.
316
317
- 318 Heikes, B. G., et al. (2002), Atmospheric methanol budget and ocean implication, *Global Biogeochem.*
319 *Cycles*, *16*(4), 1133, doi:10.1029/2002gb001895.
320
321
- 322 Hornbrook, R. S., et al. (2011), Observations of volatile organic compounds during ARCTAS –
323 Part 1: Biomass burning emissions and plume enhancements, *Atmos. Chem. Phys. Discuss.*,
324 *11*(5), 14127-14182, doi:10.5194/acpd-11-14127-2011.
325
326
- 327 Jacob, D. J., et al. (2002), Atmospheric budget of acetone, *J. Geophys. Res.*, *107*(D10), 4100,
328 doi:10.1029/2001jd000694.
329

330
331 Jacob, D. J., et al. (1996), Origin of ozone and NO_x in the tropical troposphere: A photochemical analysis
332 of aircraft observations over the South Atlantic basin, *J. Geophys. Res.*, 101(D19), 24235-24250,
333 doi:10.1029/96jd00336.
334
335
336 Johnson, M. T. (2010), A numerical scheme to calculate temperature and salinity dependent air-water
337 transfer velocities for any gas, *Ocean Sci.*, 6(4), 913-932, doi:10.5194/os-6-913-2010.
338
339
340 Lelieveld, J., et al. (2002), Global Air Pollution Crossroads over the Mediterranean, *Science*, 298(5594),
341 794-799, doi:10.1126/science.1075457.
342
343
344 Lewis, A. C., et al. (2005), Sources and sinks of acetone, methanol, and acetaldehyde in North Atlantic
345 marine air, *Atmos. Chem. Phys.*, 5(7), 1963-1974, doi:10.5194/acp-5-1963-2005.
346
347
348 Liss, P. S., et al. (1974), Flux of gases across the air-sea interface, *Nature*, 247(January 25, 1974), 181-
349 184.
350
351
352 Mao, H., et al. (2006), Controls on methanol and acetone in marine and continental atmospheres,
353 *Geophys. Res. Lett.*, 33(2), L02803, doi:10.1029/2005gl024810.
354
355
356 Mao, J., et al. (2010), Chemistry of hydrogen oxide radicals (HO_x) in the Arctic troposphere in spring,
357 *Atmos. Chem. Phys.*, 10(13), 5823-5838, doi:10.5194/acp-10-5823-2010.
358
359
360 Marandino, C. A., et al. (2005), Oceanic uptake and the global atmospheric acetone budget, *Geophys.*
361 *Res. Lett.*, 32(15), L15806, doi:10.1029/2005gl023285.
362
363
364 Marandino, C. A., et al. (2006), Correction to Oceanic uptake and the global atmospheric acetone budget,
365 *Geophys. Res. Lett.*, 33(24), L24801, doi:10.1029/2006gl028225.
366
367
368 Mopper, K., et al. (1986), Sources and sinks of low molecular weight organic carbonyl compounds in
369 seawater, *Marine Chemistry*, 19(4), 305-321.
370
371
372 Murphy, J. G., et al. (2010), Measurements of volatile organic compounds over West Africa, *Atmos.*
373 *Chem. Phys.*, 10(12), 5281-5294, doi:10.5194/acp-10-5281-2010.
374
375
376 Nemecek-Marshall, M., et al. (1995), Marine *Vibrio* species produce the volatile organic compound
377 acetone, *Applied and Environmental Microbiology*, 61(44-47).
378

379
380 Nightingale, P. D., et al. (2000), In situ evaluation of air-sea gas exchange parameterizations using novel
381 conservative and volatile tracers, *Global Biogeochem. Cycles*, *14*(1), 373-387,
382 doi:10.1029/1999gb900091.
383
384
385 Sander, S. P., et al. (2011), Chemical kinetics and photochemical data for use in atmospheric studies:
386 Evaluation number 17*Rep.*, Jet Propulsion Laboratory, Pasadena, California.
387
388 Singh, H., et al. (2000), Distribution and fate of selected oxygenated organic species in the troposphere
389 and lower stratosphere over the Atlantic, *J. Geophys. Res.*, *105*(D3), 3795-3805,
390 doi:10.1029/1999jd900779.
391
392
393 Singh, H. B., et al. (1995), High concentrations and photochemical fate of oxygenated hydrocarbons in
394 the global troposphere, *Nature*, *378*, 50-54.
395
396
397 Singh, H. B., et al. (2009), Chemistry and transport of pollution over the Gulf of Mexico and the Pacific:
398 spring 2006 INTEX-B campaign overview and first results, *Atmos. Chem. Phys.*, *9*(7), 2301-
399 2318, doi:10.5194/acp-9-2301-2009.
400
401
402 Singh, H. B., et al. (2001), Evidence from the southern Pacific troposphere for large global abundances and
403 sources of oxygenated organic compounds, *Nature*, *410*, 1078-1081.
404
405
406 Singh, H. B., et al. (1994), Acetone in the atmosphere: Distribution, sources, and sinks, *J. Geophys. Res.*,
407 *99*(D1), 1805-1819, doi:10.1029/93jd00764.
408
409
410 Singh, H. B., et al. (2003), Oxygenated volatile organic chemicals in the oceans: Inferences and
411 implications based on atmospheric observations and air-sea exchange models, *Geophys. Res.*
412 *Lett.*, *30*(16), 1862, doi:10.1029/2003gl017933.
413
414
415 Singh, H. B., et al. (2004), Analysis of the atmospheric distribution, sources, and sinks of oxygenated
416 volatile organic chemicals based on measurements over the Pacific during TRACE-P, *J. Geophys.*
417 *Res.*, *109*(D15), D15S07, doi:10.1029/2003jd003883.
418
419
420 Sinha, V., et al. (2007), Air-sea fluxes of methanol, acetone, acetaldehyde, isoprene and DMS from a
421 Norwegian fjord following a phytoplankton bloom in a mesocosm experiment, *Atmos. Chem.*
422 *Phys.*, *7*(3), 739-755, doi:10.5194/acp-7-739-2007.
423
424
425 Taddei, S., et al. (2009), Carbon Dioxide and Acetone Air–Sea Fluxes over the Southern Atlantic,
426 *Environmental Science & Technology*, *43*(14), 5218-5222, doi:10.1021/es8032617.
427

428
429 van der Werf, G. R., et al. (2009), Estimates of fire emissions from an active deforestation region in the
430 southern Amazon based on satellite data and biogeochemical modelling, *Biogeosciences*, 6(2),
431 235-249, doi:10.5194/bg-6-235-2009.
432
433
434 van Donkelaar, A., et al. (2008), Analysis of aircraft and satellite measurements from the Intercontinental
435 Chemical Transport Experiment (INTEX-B) to quantify long-range transport of East Asian sulfur
436 to Canada, *Atmos. Chem. Phys.*, 8(11), 2999-3014, doi:10.5194/acp-8-2999-2008.
437
438
439 van het Bolscher, M., et al. (2008), REanalysis of the TROpospheric chemical composition over the past
440 40 years: A long-term global modeling study of tropospheric chemistry funded under the 5th EU
441 framework programme Rep. EU-Contract No. EVK2-CT-2002-00170, 1-77 pp, MPI for
442 Meteorology, Hamburg, Germany.
443
444 Warneke, C., et al. (2001), Organic trace gas composition of the marine boundary layer over the
445 northwest Indian Ocean in April 2000, *Atmospheric Environment*, 35(34), 5923-5933.
446
447
448 Wild, O., et al. (2000), Fast-J: Accurate simulation of in- and below-cloud photolysis in Tropospheric
449 Chemical Models, *Journal of Atmospheric Chemistry*, 37, 245-282.
450
451
452 Williams, J., et al. (2004), Measurements of organic species in air and seawater from the tropical Atlantic,
453 *Geophys. Res. Lett.*, 31(23), L23S06, doi:10.1029/2004gl020012.
454
455
456 Zhou, X., et al. (1997), Photochemical production of low-molecular-weight carbonyl compounds in
457 seawater and surface microlayer and their air-sea exchange, *Marine Chemistry*, 56(3-4), 201-213.
458
459
460
461